Available online at www.sciencedirect.com
SCIENCE DIRECT®
Journal of Chromatography A, 1074 (2005) 89–98
JOURNAL OF CHROMATOGRAPHY A
www.elsevier.com/locate/chroma

Full verification of the liquid exclusion-adsorption chromatography theory using monolithic capillary columns

Frédéric Lacharme, Véronique Lapeyre, Valérie Ravaine *

Laboratoire d'Analyse Chimique par Reconnaissance Moléculaire (LACReM), ENSCPB, 16 Av Pey Berland, 33607 Pessac, France

Received 4 October 2004; received in revised form 11 March 2005; accepted 14 March 2005

Abstract

Capillary electrochromatography (CEC) was used to separate alkyl phenol ethoxylates (APEs) as model diblock copolymers, with monolithic polymers as stationary phases. The order of elution indicate that the two polymer blocks follow distinct chromatographic modes: size-exclusion for the poly(oxyethylene) group and adsorption interaction for the alkyl part. Therefore, our experimental results were compared to the theory describing liquid exclusion-adsorption chromatography (LEAC). They were found in perfect agreement with the theory, which turned to be verified for the first time over the full range of polymer lengths.

Keywords: Capillary electrochromatography; Liquid exclusion-adsorption chromatography; Alkyl phenol ethoxylates; Monoliths

1. Introduction

The characterization of polymers represents a demanding analytical task, owing to the intrinsic complexity of these materials. Polymer samples appear rarely as unique compounds but mostly as mixtures of many compounds. A single polymer molecule is built up from one or a few different repeat units, which can be arranged following different architectures or different number of repeating units. Therefore, the complexity arises from the possibility to simultaneously combine different distributions. The most common technique used to separate different constituents within a polymer blend is size-exclusion chromatography (SEC), which allows to discriminate between different molar masses [1,2]. Although this technique gives many satisfying results, it shows severe limitations in the area of functional (block-, random or grafted-) polymers as it does not account for other distributions like functionality, chemical composition or architecture. Consequently, a complete characterization of a polymer sample requires at least a two-dimensional separation technique [3], where chemical and molar mass distribution can be deconvoluated based on different separation mechanisms.

Two main separation mechanisms have been identified in liquid chromatography: size-exclusion chromatography (SEC) where polymers are separated according to their molecular size, and liquid adsorption chromatography (LAC), which separates according to the number of structural units capable of being adsorbed on the stationary phase. At the frontier between these two modes, a third limiting case is called the LC at the critical point of adsorption or under critical conditions (LCCC). Under these conditions, all chains bearing the same repeating unit elute at the same elution volume regardless of their length. A comprehensive theoretical description of homopolymers separation was reported by Gorbunov and Skvortsov [4]. More recently, this theory was extended to the case of diblock copolymers separation, for which one block may follow the LAC mode, whereas the second block is excluded [5]. This theory, called liquid exclusion-adsorption chromatography (LEAC) was partially verified experimentally using fatty alcohol ethoxylates (FAEs) [6].

The aim of this paper is to give further insight in the fundamental mechanisms underlying polymer separation. Therefore, the separation of diblock copolymers or oligomers

* Corresponding author. Tel.: +33 5 40 00 27 30; fax: +33 5 40 00 27 17.
E-mail address: v.ravaine@enscpb.fr (V. Ravaine).

0021-9673/$ – see front matter © 2005 Elsevier B.V. All rights reserved.
doi:10.1016/j.chroma.2005.03.112

was investigated using capillary monolithic columns. Such phases have recently received considerable attention as an attractive alternative to particulate materials, displaying good chromatographic performances in addition to a good control over their porous properties and surface chemistry [7,8]. Both electrically and pressure-driven separations can be achieved using these phases, but the second is restricted to rigid monoliths with strong mechanical properties, which are able to withstand high pressures. Therefore, our attention turned towards capillary electrochromatography (CEC), which offers the use of a broader range of monoliths.

In addition, using CEC to separate diblock copolymers was a way to further increase the knowledge concerning the applications of this recent technique. In the area of macromolecules, this technique has yet proved its interest concerning biological species like proteins or peptides [9], but it has poorly been explored in the area of synthetic polymers [10–13]. On a fundamental point of view, it is worth understanding separation mechanisms of large molecules in electrochromatographic mode. Up to now, the separation of synthetic polymers by electrochromatography was mainly reported by Kok and co-workers [14–16], who investigated the separation of various chemical structures of homopolymers on packed capillaries. Their main goal was to explore the capabilities of electrochromatography to discriminate between different molecular weights within a polymer family, i.e. the size-exclusion mode of electrochromatography (size-exclusion chromatography, SEEC). Another example of polymer separation was also reported to show the potentiality of a monolithic stationary phase [17].

In this paper, we report on the separation of diblock copolymers or oligomers using monolithic stationary phases. Alkyl phenol ethoxylates (APEs) were chosen as a model since they were UV-detectable. Two types of polymeric materials were used, bearing a different crosslinking density. The poorly crosslinked phase, based on poly-(*N*-isopropylacrylamide) (PNIPAM), consists of a swollen network, whereas the highly cross-linked one looks like a porous solid phase with a well-defined pore size. In each case, various separation conditions were investigated and the order of elution always corresponded to a LEAC mode. Therefore, our experimental results were compared to the theoretical predictions. Our results were in good agreement with the theory and gave the first experimental data covering the whole range of theoretical prediction. The influence of the chromatographic support was also evaluated.

2. Experimental

2.1. Materials (ou chemicals)

N-Isopropylacrylamide (NIPAM), 2-acrylamido-2-methyl-1-propanesulfonic acid (AMPS), ammonium persulfate (APS), *N*,*N*,*N*′,*N*′-tetramethylenediamine (TEMED), [3-(methacryloyloxy)propyl]-trimethoxysilane, boric acid, Tris(hydroxymethyl)aminomethane (TRIS), butyl methacrylate (BuMA), ethyleneglycoldimethacrylate (EGDMA), azobisisobutyronitrile (AIBN), 1-propanol, 1,4-butanediol, sodium hydrogenophosphate, disodium phosphate were purchased from Aldrich. *N*,*N*′-Methylenebisacrylamide (BIS) was bought from BioRad Laboratories. Acetonitrile (ACN), HPLC grade was from Merck Chemicals.

2.2. Stationary phase synthesis

2.2.1. Capillary preparation

Fused-silica tubing (Polymicro) with an internal diameter (i.d.) of 100 μm and 375 μm outer diameter (o.d.) were used as the separation capillaries. An optical window for UV was created by burning a part of the polyimide layer. The inner wall of the capillary was then treated with a 1N sodium hydroxide (statically, 2 × 15 min), flushed with a 0.1N hydrochloric acid for 30 min and finally rinsed with water for 30 min. The rinsing procedure was carried out using a suction device coupled to the tap water providing vacuum. A solution of [3-(methacryloyloxy)propyl]-trimethoxysilane in acetone (50 wt.%) was introduced and left inside the capillary for 2 × 20 min. The capillary was then rinsed with acetone and water.

2.2.2. Hydrogel phase synthesis

Our strategy was to synthesize a swollen gel stationary phase capable to achieve separations based on hydrophobic interaction. As reported by Fujimoto et al. [18] and confirmed by us, a charged NIPAM-based gel completely fullfilled this requirement. NIPAM was the monomer responsible for hydrophobic interaction with solutes. The presence of charges was necessary to achieve electroosmotic flow [19]. A pregel solution was obtained by introducing 80 mg of NIPAM as the main hydrophobic monomer, 10 mg of BIS as a crosslinker, and 6 mg of AMPS as a charged monomer, in 2 mL of Tris/boric acid (100 mM/150 mM) buffer. This particular composition was chosen regarding the results obtained in a previous study which studied the influence of gel composition on alkylphenones separation [20]. The pregel solution was first degassed with argon. The polymerisation was initiated by introducing 10 μL of APS in water (10 wt.%) and 10 μL of TEMED in water (10 vol.%), and rapidly sucked into a fused-silica capillary, which had been previously treated with [3-(methacryloyloxy)propyl]-trimethoxysilane. The polymerisation proceeded overnight at room temperature.

Before use, a few centimeters sections at the capillary end were removed. The 40-cm long capillary (34 cm from inlet end to the detection window) was mounted on a cassette and was subsequently conditioned for 3 h with a 100–150 mM Tris/boric acid buffer (pH 8.2) at 8 kV (E = 200 V/cm). The capillary was ready for use when the current stayed stable.

2.2.3. Rigid monolithic phase synthesis

Porous highly crosslinked polymers, so-called monoliths, have been widely used as separation medium in

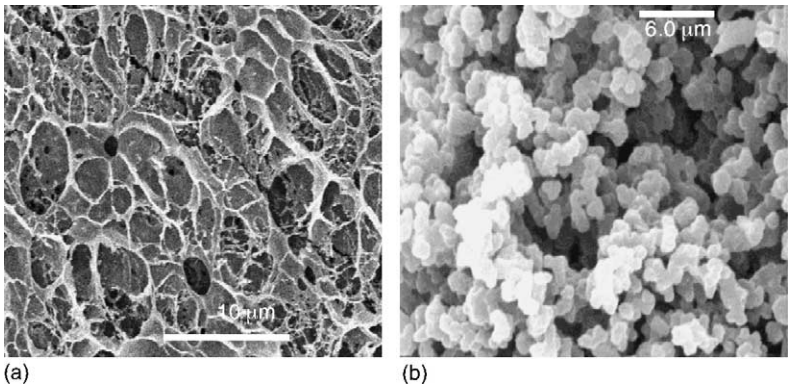

Fig. 1. SEM images of the stationary phases: (a) hydrogel after freeze-drying, scale bar: 10 μm; (b) rigid monolith with an average porous diameter of 950 nm (obtained with 59.6% of 1-propanol), scale bar: 6 μm.

electrochromatography [7]. Compared to gels, they display good mechanical properties and can support a wide range of solvents. Rather, the pionneering work of Frechet and co-workers a few years ago [21,22] showed that their porous properties could be finely tuned by carefully controlling the synthesis conditions. One major parameter is the nature of the solvent and its affinity for the growth of polymeric chains [23]. Larger pores were obtained in a poor solvent due to an earlier onset of phase separation. We used the same polymerization procedure as described previously [22]. AIBN was added to a mixture of containing 40 wt.% of monomers and 60 wt.% of solvent. The monomers mixture contained itself BuMA (60 wt.%) as a hydrophobic monomer and EGDMA (40 wt.%) as a crosslinker. The solvent mixture is made of *X* wt.% 1-propanol, *Y* wt.% 1,4-butanediol and 10 wt.% of water containing AMPS as a charged monomer. The amount of AMPS was 0.3% of the total weight. Four monoliths were obtained in this way, using the percentage *X* of 1-propanol (good solvent) varying between 58 and 62%. The mixture was deaerated by purging with argon. It was then injected in the pretreated capillary using a seringe tightly connected to the capillary, until the meniscus reached the optical window. The two ends of the capillary were connected together via a piece of plastic tubing and the capillary was immersed in a water bath at 60 °C to proceed radical polymerization for 20 h. The rest of the mixture was placed in a polyethylene vial and was also polymerized in the same conditions.

The bulk polymerized cylinder was Soxhlet extracted with methanol for 20 h to remove unreacted monomers and solvent and vacuum dried at 60 °C overnight. After cutting a small part of the extremities, the resulting capillary was connected to a HPLC pump and washed first with methanol for 30 min, then with a mixture water/methanol for the next 30 min, and finally with the mobile phase (acetonitrile and 10 mmol/L, pH 7 phosphate buffer (80:20, v/v)). The capillary length was reduced to 36 cm (29 cm active length). The capillary was then transferred to the electrophoresis instrument and equilibrated by applying a voltage of 20 kV at 25 °C, while pressurizing both inlet and outlet ends to 0.8 MPa.

2.3. Stationary phase characterization

2.3.1. Physical properties

The gel and monolith morphologies were investigated by scanning electron microscopy (JEOL JSM-5200, operating at 25 kV). The gel samples were first lyophilized. Prior to observation, all samples were gold coated using a metallizer (Technics Hummer Jr.). Typical SEM images are shown on Fig. 1. The porous properties of the rigid monolithic phases were investigated using a mercury porosimeter (Micromeritics Autopore IV 9500). The monoliths had a median pore diameter comprised between 580 and 1400 nm, with a very narrow size distribution, as shown on Fig. 2.

2.3.2. Electrochromatographic performances

Electrochromatographic experiments were carried out using a Spectraphoresis Ultra capillary electrophoresis from ThermoSeparation Products (Thermofinnigan, France) equipped with UV 3000 detector system. Data acquisition were performed using the Chromquest software.

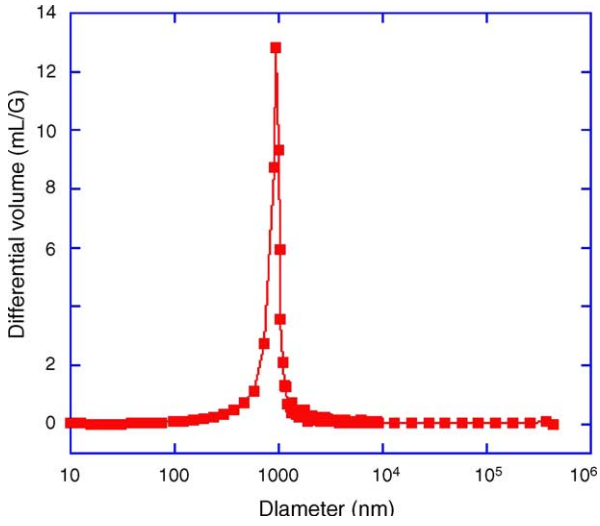

Fig. 2. Differential pore size distribution profile of a porous monolith obtained with 59.6% of 1-propanol.

For the gel phase, the mobile phase was a 100/150 mmol/L Tris/boric acid buffer (pH 8.2) mixed with different concentrations of acetonitrile. The highest amount of ACN that could be used with a gel column was 50% (v/v). Indeed, above this value, the gel collapsed and no transport across the gel was possible. The collapsed gel acted as an impermeable barrier to any ionic or molecular species.

The good quality (reproducibility, ageing) of the gel was verified by separating a mixture of test compounds (alkylphenones), using a 20:80 (v/v) ACN/buffer mobile phase, under 8 kV at 25 °C. Thiourea (TU) was used as an unretained marker. The solutes were injected electrokinetically for 3 s at a constant potential of 5 kV. An example of this separation is given on Fig. 3. Although a poor resolution was obtained with these compounds, the order of elution shows that the separation is based on a reverse-phase mode, as already stated by Fujimoto et al. [18]. The gel displayed a very stable behaviour since no deviation of elution times appeared even after 300 h of utilisation.

A similar test was performed on rigid monolithic columns. These columns allow the use of less polar mobile phases than the ones used for gels. The mobile phase was a mixture of acetonitrile and 10 mmol/L, pH 7 phosphate buffer (80:20, v/v). The test compounds were alkyl benzene derivatives, injected electrokinetically for 5 s at 5 kV and separated under 20 kV at 25 °C. Again, thiourea was used as an unretained marker. Both inlet and outlet ends were pressurized under 0.8 MPa. An example of their separation is shown on Fig. 4. In this case, a baseline resolution was achieved. It is worth noting the efficiency for thiourea was twice as much in the case of monoliths (N = 27 000) than in the case of gels (N = 12 000).

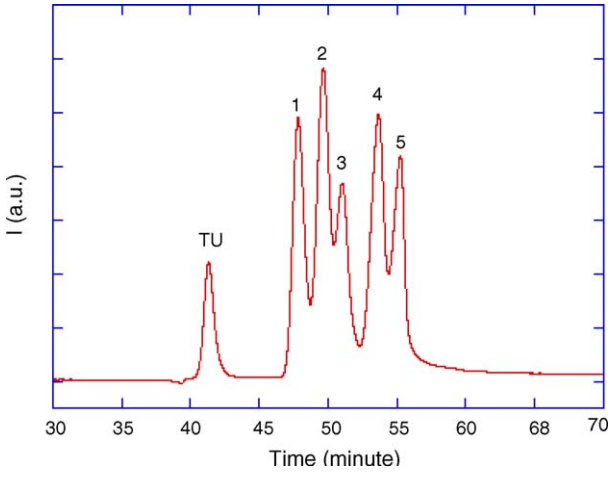

Fig. 3. Separation of alkylphenones on a hydrogel phase. Conditions: capillary, 40 cm (34 cm effective length) 0.1 mm i.d.; applied voltage, 8 kV, 7.5 μA; injection, 5 kV, 3 s; detection, UV absorbance at 254 nm; temperature, 25 °C; mobile phase 20% (v/v) acetonitrile in buffer, 100 mM Tris/150 mM boric acid (pH 8.2); sample concentration, 1–5 mM. Peaks: thiourea (TU), acetophenone (1), propiophenone (2), isobutyrophenone (3), 2-hydroxy-acetophenone (4), 2-hydroxypropiophenone (5).

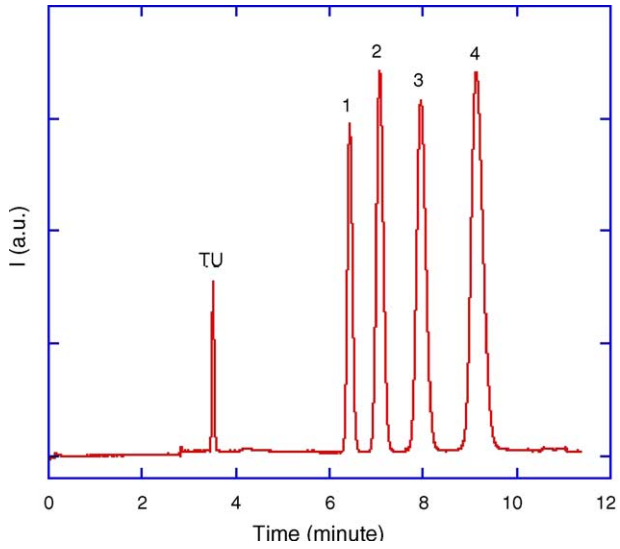

Fig. 4. Separation of alkylbenzenes on a monolithic phase. Conditions: capillary, 34 cm (29 cm effective length), 0.1 mm i.d.; applied voltage, 20 kV, 6 μA; pressure in vials, 0.8 MPa; injection, 5 kV, 5 s; detection, UV absorbance at 254 nm; temperature, 25 °C; mobile phase 80% (v/v) acetonitrile in buffer, 10 mM phosphate buffer (pH 7.2); sample concentration, 1–5 mM. Peaks: thiourea (TU), toluene (1), ethylbenzene (2), propylbenzene (3), butylbenzene (4).

2.4. Alkylphenol ethoxylates separations

Alkyl phenol ethoxylates (APEs) have a chemical structure close to fatty alcohols ethoxylates (FAEs), a very important family of nonionic surfactants. These products often consist of different polymer homologous series having the general formula presented on Fig. 5. Their structure is basically a diblock polymer structure: the first block is the alkyl chain of varying length m, noted C_m, while the second block is the poly(oxyethylene) chain of varying length n, noted E_n. For reading simplicity, they will be designed as C_mE_n. The following polydisperse APEs were used in these investigations (specifications given by the producer Aldrich). Their trade name and corresponding lengths are reported in Table 1. It should be noted that m is a perfectly defined value, whereas n corresponds to a distribution. The value reported in the table corresponds to the main component. Two homologous series of compounds were distinguished: series C_8E_n and series C_9E_n, which differ from their alkyl block length.

We used mixtures of ACN and aqueous buffer as mobile phases, with the background electrolyte respective of each type of column as mentioned above. The separation was achieved in the same experimental conditions as those for the test compounds, except for the detection wavelength, which

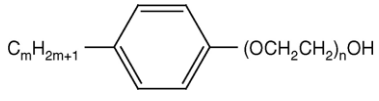

Fig. 5. Structure of the alkylphenol ethoxylates C_mE_n.

Table 1
Summary of the studied APEs samples

Name	*m*	*n*
Igepal CA-210	8	2
Igepal CA-520	8	5
Igepal CA-630	8	9
Triton X-405	8	40
Igepal CO-210	9	2
Igepal CO-520	9	5
Igepal CO-720	9	12
Igepal CO-890	9	40
Igepal CO-990	9	100

Trade name and corresponding C_mE_n composition of the main component.

was chosen at 226 nm. We checked that the current never exceeded 10 μA, and therefore, avoided any unwanted Joule heating. No effort was made to optimize other separation parameters such as electrolyte concentration, pH, or temperature, although it was shown very recently that they could improve both the resolution and efficiency of the separation of APEs [24].

3. Theoretical considerations

The following section is a summary of the main aspects of the theory developed by Trathnigg et al. [5] and Trathnigg and Gorbunov [6] for diblock copolymers separation.

When a polymer chain travels within a channel or a pore, it may adopt different behaviours depending on its chemical composition, its length, the nature of the solvent, the size of the pore and the nature of its surface. At a macroscopic level, the relevant value in liquid chromatography is the elution volume, which has the following definition for a packed bed column:

$$V_e = V_i + KV_p \quad (1)$$

where V_i denotes interstitial volume (outside the particles) and V_p, the pore volume inside the particles. K is the distribution coefficient related to the equilibrium between the solute at the surface and in the mobile phase. It is related to the variation in Gibbs free energy associated to the transition from the mobile phase to the stationary phase. The Gibbs free energy is itself divided into two contributions: enthalpy and entropy. The elution mode results from a competition between these two contributions.

3.1. Size-exclusion mode (SEC)

This mode is governed by entropy. The entropy loss is due to the conformational change of a polymer chain, described as a random coil with a radius of gyration R moving in a pore with a diameter d. As first described by Casassa and Tagami [25], for small molecules and wide pores ($R/d \ll 1$), K_{SEC} is given by:

$$K_{SEC} \approx 1 - \frac{2}{\sqrt{\Pi}}\frac{R}{d} \quad (2)$$

For Gaussian chains of molecular weight M, R is proportional to $\sqrt{M}$ and the relation becomes:

$$K \approx 1 - A\sqrt{M} \quad (3)$$

where A is a constant.

The elution order of the molecules will be inverted compared to their molecular mass.

3.2. Adsorption mode (LAC)

In this mode, the enthalpic contribution due to the adsorption of a polymer chain on the surface of a pore is favourable and counterbalances the loss of conformational entropy. The polymer tends to extend on the surface. The parameter of adsorption interaction c is introduced: it has the dimension of an inverse length and the value $H = c^{-1}$ is equal to the mean thickness of the layer formed by the polymer chain on a pore wall. In the asymptotic regime where the polymer radius R is large compared to H or c^{-1} ($Rc \gg 1$), the equilibrium value K_{LAC} is expressed as:

$$K_{LAC} \approx \frac{2}{cd}\exp(c^2R^2) \quad (4)$$

On a practical point of view, c varies as a function of interactions between three components: the polymer chain, the solvent (eluent), and the stationary phase. Increasing the amount of good solvent will decrease the adsorption parameter. This solvent is also called *desorli* and opposed to *adsorli*, which is a poor solvent of the polymer [26–28].

At the frontier between the LAC mode and the SEC mode, is the mode at the critical point of adsorption, called liquid chromatography under critical conditions (LCCC). Enthalpic interactions perfectly compensate the loss of conformational entropy and K is equal to 1.

3.3. Liquid exclusion-adsorption chromatography

This mode is applied to diblock copolymers made of blocks presenting opposite behaviour. Typically, block A is adsorbed on the surface of the pore, whereas block B is excluded (Fig. 6). Theoretical results have been established in the general approximation that R_A and R_B are both much more smaller than the pore diameter d. In the special situation where the block A is strongly adsorbed, the constant

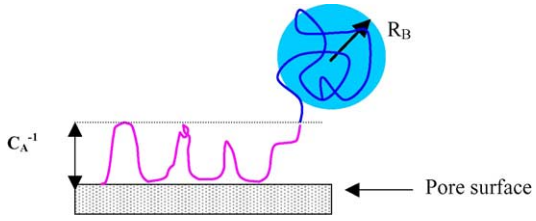

Fig. 6. Schematic representation of the chromatographic behaviour of a diblock copolymer constituted with two blocks displaying opposite behaviours: block A is adsorbed whereas block B is excluded.

K_{LEAC} relative to the copolymer free enthalpy change, can be written as follows:

$$K_{LEAC} = K_A Y(c_A; R_B) \quad (5)$$

where K_A is very large ($K_A \gg 1$) and constant when the length of block A is constant. K_A has the form of Eq. (4). Y is a mathematical function defined as $Y \equiv \exp(x^2)\mathrm{erfc}(x)$. It describes the behaviour of the excluded block, which depends not only on R_B but also on c_A. Two asymptotic cases can easily be calculated.

When the non-adsorbing block is small compared to the thickness of the adsorbed layer ($R_B c_A < 1$),

$$K_{LEAC} \approx K_A \left[1 - \frac{\sqrt{\Pi}}{2} c_A R_B\right] \approx K_A(1 - \tilde{C}\sqrt{N_B}) \quad (6)$$

Thus, K_{LEAC} has a linear evolution versus the square root of the number of units in the block B, which is similar to the SEC mode. The difference is that the values of K_{LEAC} are more than unity which is characteristic of an adsorption mode.

When the non-adsorbing block is large enough ($R_B c_A \gg 1$),

$$K_{LEAC} = K_A \frac{1}{\sqrt{\Pi}} \frac{1}{R_B c_A} \approx K_A \frac{1}{\tilde{C}'\sqrt{N_B}} \quad (7)$$

The linearity of K_{LEAC} is expected versus the inverse of the square root of N_B.

We point out the pore size dependence of K_{LEAC}. K_{LEAC} is proportional to K_A, which is itself inversely proportional to d, as mentioned for a LAC mode.

4. Results and discussion

4.1. Separation of alkyl phenol ethoxylates with hydrogel phase

Our strategy was to evaluate the functionality distribution of diblock copolymers using CEC. The following methodology was used. The mobile phase was a mixture of aqueous buffer and acetonitrile. Regarding the structure of these diblock molecules, it was expected that the alkyl block would adsorb on the stationary phase via hydrophobic interactions. It was also known from previous studies [29] that acetonitrile was a good solvent of poly(oxyethylene) homopolymers whereas water promoted adsorption on a hydrophobic column. In order to avoid any irreversible adsorption of the polymer chains, we started our first analysis with the highest amount of solvent that would disfavour the adsorption of any of the blocks, which is acetonitrile. The first experiments were performed with a mobile phase constituted with 50% (v/v) of acetonitrile.

The effect of the ethoxylate chain length was compared in each series C_8E_n and C_9E_n. Fig. 7 shows an example of separation obtained for one alkyl chain length and different values of EO block length. Each sample was eluted as a single

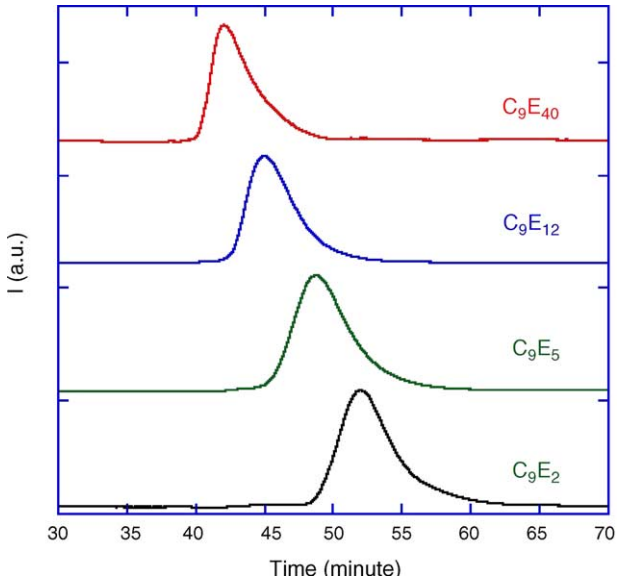

Fig. 7. Electrochromatograms showing the effect of the EO-block chain length n on the retention time of several mixtures of C_9E_n (the names indicated on the graph represents the main constituent of the distribution). The separations are performed on the hydrogel phase in 50% (v/v) acetonitrile–buffer: detection, UV absorbance at 226 nm (other conditions: see Fig. 3).

broad peak. The order of peaks was inversely proportional to the EO block length, which corresponded to a size-exclusion mode. We also investigated the role of the alkyl chain length by comparing series C_8E_n and C_9E_n with the same mobile phase (Fig. 8). Increasing the alkyl chain length increased

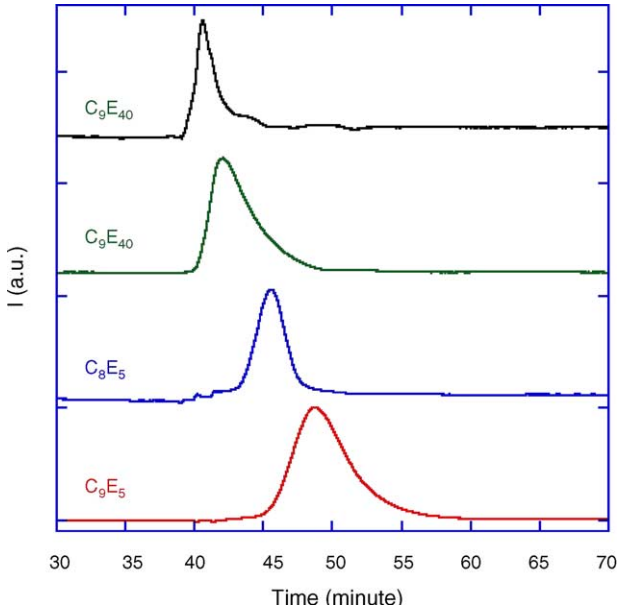

Fig. 8. Electrochromatograms showing the effect of the alkyl chain length m on the retention time of several C_mE_n (the names indicated on the graph represent the main constituent of the distribution). The separations are obtained on the hydrogel phase in 50% (v/v) acetonitrile–buffer: detection, UV absorbance at 226 nm (other conditions: see Fig. 3).

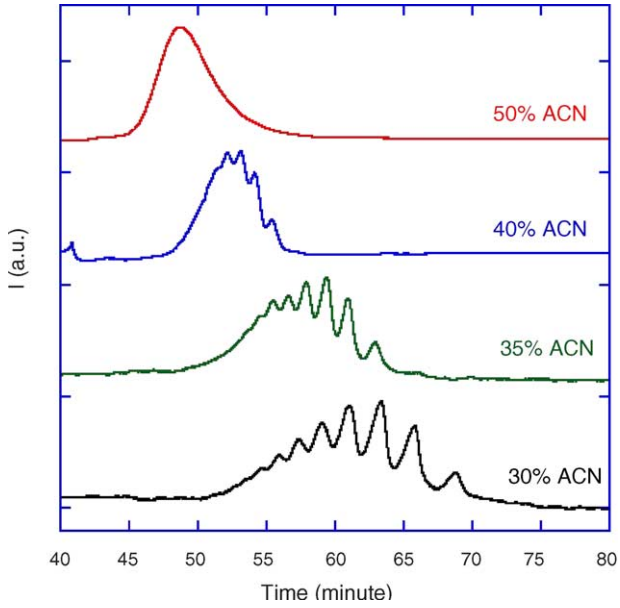

Fig. 9. Electrochromatograms showing the effect of the ACN volume fraction on the separation of Igepal CO-520 (main component C_9E_5), on the hydrogel phase. Separation conditions: detection, UV absorbance at 226 nm (other conditions: see Fig. 3).

elution times. Therefore, we could conclude that the alkyl chain was adsorbed, even at 50 vol.% of acetonitrile.

The amount of acetonitrile was progressively decreased in the mobile phase. The broad elution peaks progressively enlarged and separated into finely resolved peaks (Figs. 9 and 10). Instead of an average value of n, each peak

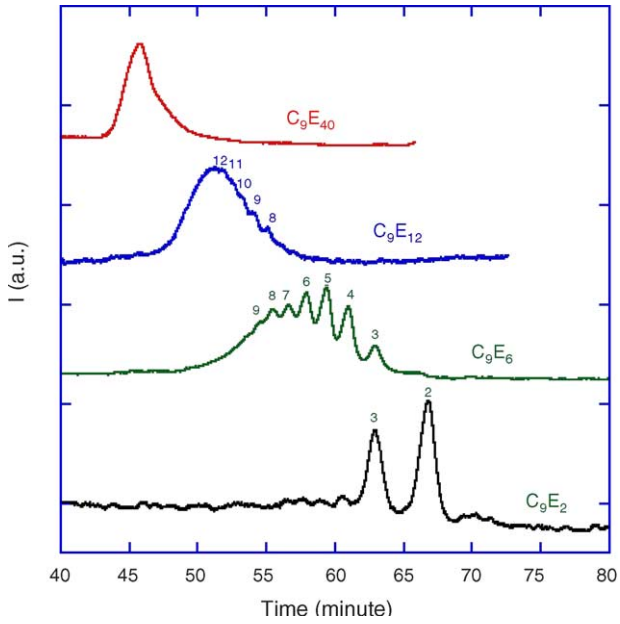

Fig. 10. Electrochromatograms showing the effect of the EO-block chain length n on the retention time of several C_9E_n (the names indicated on the graph represent the main constituent of the distribution). The separations are performed on the hydrogel phase in 35% (v/v) acetonitrile–buffer: detection, UV absorbance at 226 nm (other conditions: see Fig. 3).

corresponded to a single EO length. It could be clearly seen that each sample was constituted with a mixture of several EO chain lengths. To identify the peaks, we made the assumption that the highest peak corresponded to the main component of the sample and stated that the previous peak had the value $n+1$. This assumption seemed to be correct as we found the same retention time for the same chain length n present within two different samples (Fig. 10). For example, the compound C_9E_3 is present in both samples with main constituents C_9E_5 and C_9E_2. A baseline resolution could be achieved for the smallest values of n. The order of elution indicated again a size-exclusion mode for the EO chain block. We also compared the retention times between series C_8E_n and C_9E_n, which confirmed that the alkyl chain was still adsorbed in these conditions.

The elution time of each peak could be measured and compared to the theory established for liquid chromatography. To do so, we had to estimate the values of the equilibrium constant K. In liquid chromatography, K is related to elution volumes as defined by relation (1), which is expressed for packed bed columns. In the case of monolithic columns, this relation is still valid, considering that the continuous media contain two types of pores in their structure [30–32]: (i) the larger pores, called through pores, which form the flow-channel network outside the monolith skeleton, corresponding to the interstitial volume, (ii) the smaller mesopores inside the matrix, providing the interaction with the solutes, corresponding to the porous volume. The usual way to determine these values experimentally is to separate standard polymers in a pure exclusion mode. This could not be achieved with hydrogels because we could not find a standard which could be both soluble in water rich solvents and detectable with a UV detector. Therefore, we had to express K as a function of the total void volume and the elution volume, which are the variables experimentally accessible. We define that the porous volume V_p is a small part α of the total void volume V_0, i.e. $V_p = \alpha V_0$. In this case, K is related to V_e and V_0 through the relation:

$$\alpha K = \frac{V_e}{V_0} - 1 + \alpha \tag{8}$$

In practise, we calculate the ratio between the time of elution and a time of reference t_0 instead of the ratio between the corresponding volumes. Indeed, the volume is not directly accessible in the case of CEC, since the flow velocity is an internal variable, controlled by the electroosmotic flow in the column, which is dependent of the level of charges in the stationary matrix and the ionic strength of the mobile phase. The time t_0 is the elution time of an unretained solute (thiourea), which was supposed to travel over the entire pore volume. It depended on the mobile phase composition.

To compare our results to the LEAC theory presented above, we investigated the two asymptotical regimes, where the evolution of K is predicted versus the number of units of the non-adsorbing block (the polyethylene oxide block in our case). We assumed that both R_A and R_B are smaller than

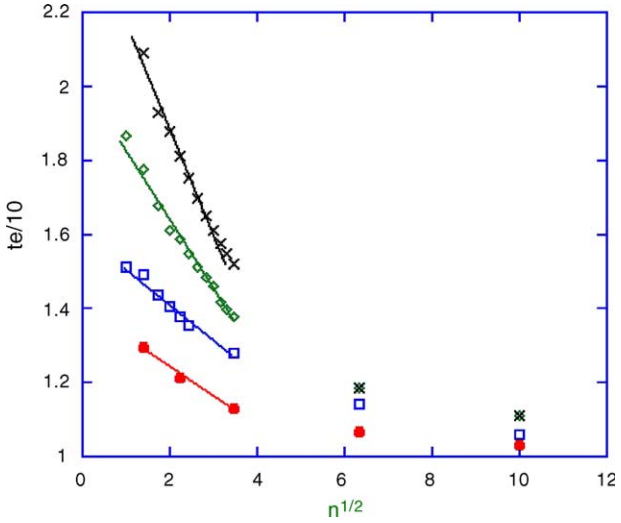

Fig. 11. Plot of t_e/t_0 as a function of $\sqrt{n}$ for the series C_9E_n on the hydrogel phase in different ACN volume fractions (vol.%): (●) 50, (□) 40, (◊) 35, (×) 30.

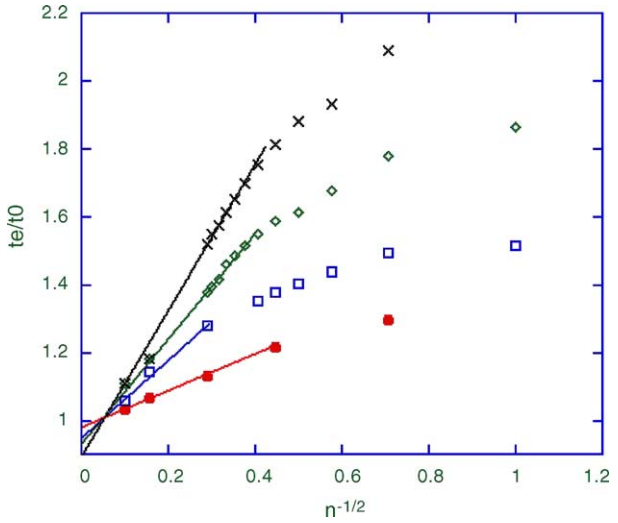

Fig. 12. Plot of t_e/t_0 as a function of $1/\sqrt{n}$ for the series C_9E_n on the hydrogel phase in different ACN volume fractions (vol.%): (●) 50, (□) 40, (◊) 35, (×) 30.

the pore diameter. We first investigated the regime where R_B is small compared to the thickness of the adsorbed layer ($R_B c_A < 1$). Our experimental values of t_e/t_0, i.e. $\alpha K + 1 - \alpha$ were plotted versus the square root of n (Fig. 11). As predicted by the theory and also experimentally obtained by Trathnigg and Gorbunov [6], it exhibited a linear evolution versus $\sqrt{n}$. This linear relation holds only in the range of small n ($n < 10$) where the gyration radius R_B is supposed to be small. Moreover, this linear behaviour is available for several mobile phase compositions and for both series C_8E_n and C_9E_n (data not shown). The slope of these lines depends on the length of the alkyl group (m) and also on the mobile phase composition. According to the theory, the slope is proportional to K_A. It increases as the volume fraction of ACN decreases and also increases as the alkyl chain length increases, which is in perfect agreement with a reverse-phase mode.

We completed our comparison with theory by investigating the other regime, where $R_B c_A \gg 1$, which corresponds to large gyration radii R_B. We plot t_e/t_0 as a function of the inverse square root of n (Fig. 12). This time, a linear portion was observed in the region of large n ($n > 6$). This indicated that the second regime of the theory was achieved for the longest chains (large R_B), in the same separation conditions as for the first regime, which means that c_A has the same value. According to the theory in Eq. (7), the slopes should be proportional to K_A/c_A. For a given mobile phase, c_A is supposed to be constant. The slope increased when increasing the chain length, which means that K_A increased, which is again in good agreement with an adsorption phenomenon. Also according to Eq. (7), K is directly proportional to $1/\sqrt{n}$ and the fit should cross the origin. Therefore, our fit of t_e/t_0 versus $1/\sqrt{n}$ should cross the y-axis in $1 - \alpha$. As shown on Fig. 12, the lines cross the y-axis close at values comprised between 0.9 and 0.98, depending on the volume fraction of ACN in the mobile phase. Therefore, α is below 10%, which is in reasonable agreement with its physical meaning. Its dependence on the mobile phase composition can be explained by the soft properties of the gel phase. Indeed, as mentioned previously, the swollen state of the gel phase depends on the nature of the solvent and thus, the porosity of the gel decreases as the volume fraction of ACN increases.

4.2. Separation of alkyl phenol ethoxylates with monolithic rigid phases

The same samples were also analyzed using the monolithic capillaries described above. The mobile phases were richer in acetonitrile than for the gel phases (from 65 to 95%, v/v). The buffer was a 10 mmol/L phosphate solution at a pH of 7. The same features as for the hydrogel phase were observed. For acetonitrile-rich mobile phases, the largest samples eluted as one broad peak and the peaks were in the order of a size-exclusion mode for the poly(oxyethylene) chain and in the order of a reverse-phase mode for the alkyl chain. When decreasing the ratio of acetonitrile, some of these peaks started to deconvoluate. However, they remain broad and no baseline resolution could be achieved. A typical chromatogram is presented on Fig. 13 for series C_9E_n in 80% acetonitrile. For the smallest values of n, each EO length could be separated even at 95% of ACN. Decreasing the ratio of ACN only increased the retention time and accentuated the asymmetrical shape of the peaks. This seems to indicate a rather stronger adsorption of these compounds on the monolithic phase. We investigated four columns having different pore size distributions but found no significant effect of the porosity on the shape of the peaks.

Although the resolution was not as good as with the gel columns, we picked the peaks position and compare the experimental values to the theory. We first plotted t_e/t_0

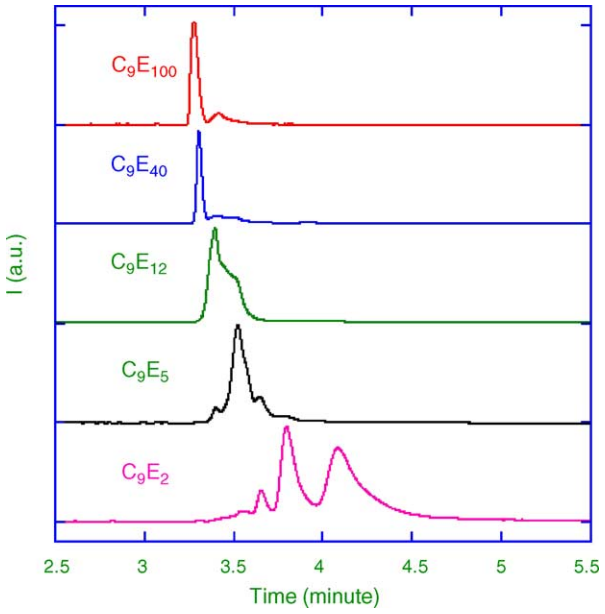

Fig. 13. Electrochromatograms of several C_9E_n (the names indicated on the graph represent the main constituent of the distribution) as obtained on a monolithic phase in 80% (v/v) acetonitrile–buffer: detection, UV absorbance at 226 nm (other conditions: see Fig. 4).

versus the square root of n. As shown on Fig. 14, the resulting curve was not linear at all. This suggested that the condition $R_B c_A < 1$ was not satisfied, probably meaning that the adsorption of the alkyl chain was rather strong (high c_A).

We explored the second asymptotic regime and plotted t_e/t_0 versus the inverse of the square root of n. A linear behaviour is observed on the whole range of n for the mobile phase containing at 85 vol.% ACN (Fig. 15). The curve crosses the y-axis in 0.92, which corresponds to a porous volume V_p occupying 8% of the total volume V_0. This order

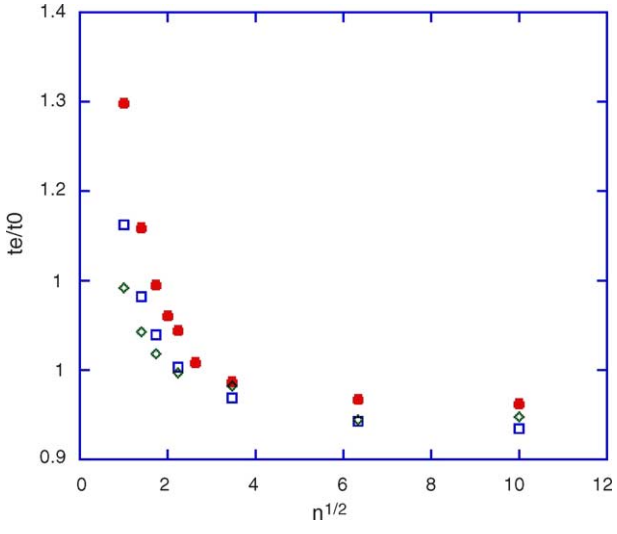

Fig. 14. Plot of t_e/t_0 as a function of $\sqrt{n}$ for the series C_9E_n on a monolithic phase in different ACN volume fractions (vol.%): (◊) 85, (□) 80, (●) 70.

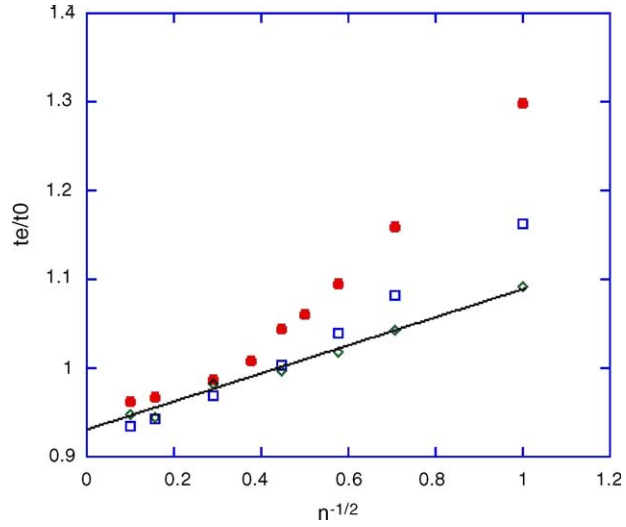

Fig. 15. Plot of t_e/t_0 as a function of $1/\sqrt{n}$ for the series C_9E_n on a monolithic phase in different ACN volume fractions (vol.%): (◊) 85, (□) 80, (●) 70.

of magnitude is similar to that obtained for gel phases. We verified that this value has a physical meaning by looking at carefully the porosity distribution profile (Fig. 2). The porous volume was defined as the smallest pores of the distribution. They can be either pores which are not visible on the porosity distribution profile, maybe smaller than 10 nm, or simply the part of the distribution corresponding to the smaller pores.

When decreasing the volume fraction of ACN, the experimental data seem to be fitted by two distinct linear domains. The first one corresponds to large n ($n > 12$), where data are almost superimposed whatever the ratio of ACN. A second linear domain appears in the range of small n ($n < 12$), which is unexpected from the theoretical considerations exposed above. Based on the assumption of a strong adsorption of the alkyl chain on the monoliths, we would have expected that a single linear regime would be observed on the whole range of n or at least for the largest n, with a slope proportional to K_A/c_A, i.e. varying with the mobile phase composition. Therefore, the LEAC theory does not seem to explain the separation of APE diblock copolymers with our rigid monoliths. The very high adsorption of the alkyl chain, as indicated by the asymmetrical shape of the peaks, may originate this particular behaviour. Further experimental data will be required to better understand this behaviour.

4.3. Comparison between hydrogel and rigid monolithic phases

From an analytical point of view, the experimental results show that the separation of alkyl phenol ethoxylates was achieved with a better resolution with a hydrogel stationary phase than with a monolithic one. This result was rather unexpected as it appeared opposite to the results obtained with small molecules, where both efficiency and resolution were

found better with rigid monoliths. Several criteria may be incriminated. Some of them concern the mobile phase and have not been investigated yet: the nature and concentration of the background electrolyte and also the pH. However, in a recent publication [24], Norton and Shamsi interested in the optimisation of the separation of one alkyl phenol ethoxylate, named Triton X-100. They showed that the parameters relative to the mobile phase could be tuned to optimise the separation but also that their impact was minor compared to the nature of the stationary phase. These authors compared different packing materials and showed that the presence of uncapped silanol groups strongly enhanced the separation of Triton X-100, possibly through H-bonding interactions. A similar conclusion may hold for our results. Indeed, the difference between soft and rigid stationary phases could be explained by their ability to induce H-bonding interactions or not. The hydrogel phases offer this possibility since they present amide functions, whereas monolithic acrylate-based materials do not. The porous structure might also play a role in the polymer separation but further information is required to conclude on this effect. To gain insight into the role of the structure, we should keep constant the chemical nature of the columns: the separation of alkyl phenol ethoxylates should be carried out with a highly crosslinked acrylamide-based polymer.

5. Conclusion

In this study, we have shown that the separation of diblock copolymers such as APEs could be obtained with monolithic columns. Moreover, this separation was achieved using CEC, which showed that this technique could be used in type of mode as defined in classical LC. The possibility to separate diblock copolymers such as alkyl phenol ethoxylates, in a mode combining adsorption and size-exclusion is a proof of its broad application range. Two kinds of chromatographic materials were investigated in this study. Soft hydrogels exhibited rather good chromatographic performances towards the separation of alkyl phenol ethoxylates, and appeared unexpectedly better than rigid monolithic polymers.

The influence of the mobile phase composition on the separation was investigated, using mixtures of acetonitrile and aqueous buffer. It was possible to separate each individual poly(oxyethylene) chain length by decreasing the amount of acetonitrile. We concluded from the order of elution that the PEO block always separated following a size-exclusion mode, whereas the alkyl group exhibited adsorption interactions. Therefore, our experimental results were compared to the LEAC theory. Results with the hydrogel phase were found to be in good agreement with the theoretical predictions. This was the first experimental verification on the full range of non-adsorbing block length.

Acknowledgements

The authors wish to thank Professor Henri Cramail for fruitful discussions about polymer analysis and Laurence Moine for porosity measurements.

References

[1] W.W. Yau, J.J. Kirkland, D.D. Bly, Modern Size Exclusion Liquid Chromatography, Wiley, 1979.
[2] H. Pasch, B. Trathnigg, HPLC of Polymers, Springer, 1997.
[3] A. Van der Orst, P.J. Schoenmakers, J. Chromatogr. A 1000 (2003) 693.
[4] A. Gorbunov, A.M. Skortsov, Adv. Colloid Interface Sci. 62 (1995) 31.
[5] B. Trathnigg, B. Maier, A. Gorbunov, A. Skvortsov, J. Chromatogr. A 791 (1997) 21.
[6] B. Trathnigg, A. Gorbunov, J. Chromatogr. A 910 (2001) 207.
[7] E.F. Hilder, F. Svec, J.M.J. Fréchet, Electrophoresis 23 (2002) 3934.
[8] C. Legido-Quigley, N.D. Marlin, V. Melin, A. Manz, N.W. Smith, Electrophoresis 24 (2003) 917.
[9] D. Bandilla, C.D. Skinner, J. Chromatogr. A 1044 (2004) 113.
[10] C.M. Johnson, A.P. McKeown, M.R. Euerby, J. Chromatogr. Library 62 (2001) 87.
[11] Y. Vender Heyden, S.T. Popovici, P.J. Schoenmakers, J. Chromatogr. A 957 (2002) 127.
[12] W.T. Kok, J. Chromatogr. A 1044 (2004) 145.
[13] K. Mistry, H. Cortes, D. Meunier, C. Schmidt, B. Feibush, N. Grinberg, I. Krull, Anal. Chem. 74 (2002) 617.
[14] F. Ding, R. Stol, W.T. Kok, H. Poppe, J. Chromatogr. A 924 (2001) 239.
[15] R. Stol, W.T. Kok, H. Poppe, J. Chromatogr. A 914 (2001) 201.
[16] R. Stol, J.L. Pedersoli, H. Poppe, W.T. Kok, Anal. Chem. 74 (2002) 2314.
[17] E.C. Peters, M. Petro, F. Svec, J.M.J. Fréchet, Anal. Chem. 70 (1998) 2296.
[18] C. Fujimoto, Y. Fujise, E. Matsuzawa, Anal. Chem. 68 (1996) 2753.
[19] V. Pretorius, B.J. Hopkins, J.D. Schieke, J. Chromatogr. 99 (1974) 23.
[20] V. Ravaine, Unpublished results.
[21] E.C. Peters, M. Petro, F. Svec, J.M.J. Frechet, Anal. Chem. 69 (1997) 3646.
[22] E.C. Peters, M. Petro, F. Svec, J.M.J. Frechet, Anal. Chem. 70 (1998) 2288.
[23] C. Viklund, F. Svec, J.M. Fréchet, Chem. Mater. 8 (1996) 744.
[24] D. Norton, S.A. Shamsi, Electrophoresis 25 (2004) 586.
[25] E.F. Casassa, Y. Tagami, Macromolecules 2 (1969) 14.
[26] S.D. Nguyen, D. Berek, Colloids Polym. Sci. 277 (1999) 318.
[27] K. Baran, S. Laugier, H. Cramail, Int. J. Polym. Anal. Charact. 6 (2000) 123.
[28] S.D. Nguyen, D. Berek, Colloids Surf. A 162 (2000) 75.
[29] K. Baran, S. Laugier, H. Cramail, J. Chromatogr. B 753 (2001) 139.
[30] F.C. Leinweber, D. Lubda, K. Cabrera, U. Tallarek, Anal. Chem. 74 (2002) 2470.
[31] M.R. Buchmeiser, Angew. Chem. Int. Ed. 40 (2001) 3795.
[32] D. Moravcova, P. Jandera, J. Urban, J. Planeta, J. Sep. Sci. 26 (2003) 1005.